

Switchable Brillouin frequency multiwavelength and pulsed fiber laser

S. J. Tan^{1,*}, H. Haris², and S. W. Harun^{2,3}

¹*School of Engineering, KDU University College, Utropolis Glenmarie, Shah Alam 40150, Malaysia*

²*Department of Electrical Engineering, Faculty of Engineering, University of Malaya, Kuala Lumpur 50603, Malaysia*

³*Photonics Research Center, University of Malaya, Kuala Lumpur 50603, Malaysia*

*Corresponding author: tsjin@yahoo.com

Received March 23, 2017; accepted June 6, 2017; posted online June 30, 2017

Switchable single and double Brillouin multiwavelength and pulsed laser is successfully demonstrated. Brillouin spacing can be switched from single (0.08 nm) to double spacing (0.16 nm) or vice versa by swapping the ports of the coupler in the proposed configuration. The proposed configuration can also be used to produce pulsed laser by inserting a home-made carbon nanotubes saturable absorber into the laser cavity. The proposed system is very versatile and flexible as it can be used as a multiwavelength laser or pulsed laser to cater for different types of applications.

OCIS codes: 140.3500, 290.5900, 190.4370.

doi: 10.3788/COL201715.101401.

Multiwavelength fiber lasers are widely used in dense wavelength division multiplexing (DWDM), optical sensing, and spectroscopy^[1,2]. Many approaches have been demonstrated to produce multiwavelength sources, such as stimulated Brillouin scattering (SBS)^[3], nonlinear polarization rotation (NPR)^[4], four wave mixing (FWM)^[5], and spectral slicing^[6]. Among all these techniques, SBS is of interest and widely used in the telecommunication industry due to its low threshold power and narrow linewidth. SBS is a nonlinear effect that arises from the interaction between the intense pump light and acoustic waves in a nonlinear medium, which results in the incident pump light to be back scattered. This SBS effect can be cascaded and subsequently generate multiple narrow Stokes lines with equal spacing. Since the first demonstration of a hybrid Brillouin erbium fiber laser (BEFL) by Cowle and Stepanov^[7], many efforts have been put forward to generate a multiwavelength comb with a constant spacing of 0.08 nm^[8,9].

Some works have also been carried out to double up the channel spacing to 0.16 nm in order to facilitate the de-multiplexing process. A double spacing multiwavelength Brillouin fiber laser (DS-MWBFL) can be realized using a four port circulator to extract out the even order Stokes^[10]. Recently, researchers paid much attention to attain a switchable Brillouin spacing fiber laser with the purpose to provide a flexible multiwavelength source in optical communication. A switchable spacing MWBFL had been demonstrated by cascading Brillouin nonlinear gain media and changing the Brillouin pump (BP) power^[11,12]. Moreover, the proposed setups in Refs. [11,12] are rather bulky, as they used two Brillouin nonlinear gains in the range of 9–25 km long. Additionally, Hu *et al.*^[13,14] demonstrated a switchable spacing MWBFL by rearranging the connection ports and using an optical switch.

Apart from demonstrating the flexibility of switchable Brillouin spacing, numerous researchers show interest and are also investigating the dynamics of pulses generated by SBS^[15–18]. The occurrence of pulsation due to SBS is unstable, and this includes periodic, quasi-periodic and chaotic oscillations. This instability is even more significant in a MWBFL of long cavities. Cavity longitudinal modes with different phases undergo gain competition and mode hopping, resulting in the generation of unstable pulses. Pulse stability can be enhanced by reducing the length Brillouin gain medium (BGM). Nevertheless, stability of pulse is still dependent on the phase relationship between the BP and Stokes waves.

On the other hand, stable *Q*-switched and mode-locked pulsed lasers have a broad range of applications from industry to communication. A *Q*-switched laser, which delivers high pulse energy, is widely used for surgery and micro-machining, while a mode-locked laser with narrow pulse width is used in optical transmission. There are numerous ways to generate a pulsed fiber laser, and the incorporation of a saturable absorber (SA) into the laser cavity is the most popular method. Carbon nanotubes (CNTs) and graphene SA are well known SAs and have been extensively investigated in the past few years^[19,20]. Newer SA materials are subsequently discovered, such as a topological insulator (TI)^[21] and black phosphorus^[22]. Furthermore, some researchers incorporated a SA in a Brillouin laser cavity to produce a Brillouin pulse^[23].

It would be great if a multiwavelength laser and stable pulsed laser could be produced from a single laser cavity, where its functionality can be switched between single and double Brillouin spacing and a pulsed laser. Contrary to the above mentioned techniques^[11,12], the Brillouin spacing switching is realized by just swapping two ports of a coupler, and the light propagation is still within the dual loop

of a laser cavity. The laser cavity can then be transformed into a pulsed laser by integrating a CNT SA into the cavity. This versatile fiber laser source, which has multiple functions, is very flexible and practical to be employed in many applications. To the best of our knowledge, this is the first demonstration of a multifunction laser, which has the capability to generate a single and double spacing Brillouin multiwavelength laser, as well as a pulsed laser within the same cavity.

The experimental setup of the proposed switchable Brillouin multiwavelength and pulsed fiber laser is schematically shown in Fig. 1. It consists of a piece of erbium-doped fiber (EDF), which is pumped by a 1480 nm laser diode via a wavelength division multiplexer (WDM), a piece of BGM, two optical circulators, two 3 dB couplers (C1 and C2), and one 10 dB coupler (C3). A narrow linewidth tunable laser source (TLS) is employed as the BP. The gain medium used is a piece of 3 m long EDF, which has an erbium ion concentration of 2000 ppm, cut-off wavelength of 980 nm and a dispersion coefficient of -21.64 ps/(nm·km) at 1550 nm. A 7.7 km long dispersion compensation fiber (DCF) with an effective mode area of $15 \mu\text{m}^2$ is used as the BGM. The configuration can be viewed as two loops cavity, where the two loops are connected together by a three port circulator and two 3 dB couplers. The optical output is extracted via port 3 of circulator 1 and the 10% port of the 10 dB coupler into the optical spectrum analyzer (OSA: Yokogawa AQ6360B), which has resolution of 0.02 nm.

Figure 1(a) depicts the configuration for the DS-MWBFL. The light propagation for the DS-MWBFL is as follows. The BP is amplified up to about 13 dBm by a commercial EDF amplifier (EDFA) before being injected into the cavity via a circulator. The BP (thin solid arrow) is coupled into the first loop of the cavity with a 3 dB coupler (Coupler 1-C1). It is then amplified again as it propagates through the EDF before it enters the BGM. Once the BP exceeds its threshold condition, the first Brillouin Stokes (BS) (thick solid arrow) will be generated in the anticlockwise direction and re-enters coupler 1. Then, 50% of the light (first BS) will propagate from port 2 into port 3 of circulator 1 (Cir 1) and characterized by OSA 1. The remaining 50% of light (first BS) will transmit from port 2 into port 3 of circulator 2 (Cir 2). The light will re-enter into the first loop of the cavity via coupler 2 and enters the BGM to produce the second BS. The second BS (thick dashed solid arrow) will propagate in the clockwise direction and then be extracted out by the 10 dB coupler (C3) into OSA 2. The residual light (second BS) enters coupler 2 (C2), circulator 2 (Cir 2), and coupler 1 (C1). This second BS will be amplified before it enters the BGM. The third BS will be generated if the threshold condition is met. The cascading process will continue as long as the Stokes exhibits sufficient power to induce SBS in the BGM. Here, OSA 1 and OSA 2 are used to monitor the odd and even order Stokes, respectively.

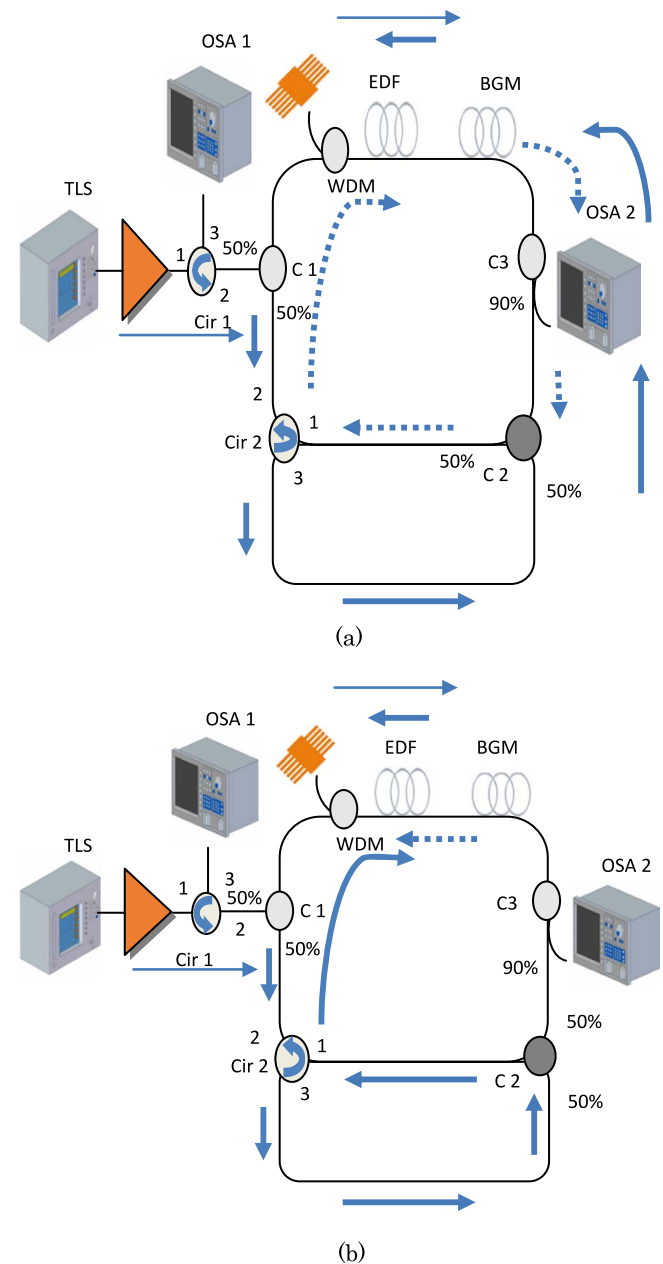


Fig. 1. Experimental setup of switchable spacing MWBFL. (a) Double Brillouin spacing: propagation of injected TLS (thin solid arrow), propagation of first BS (thick solid arrow), propagation of second BS (thick dashed arrow); (b) single Brillouin: propagation of injected TLS (thin solid arrow), propagation of first BS (thick solid arrow), propagation of second BS (thick dashed arrow).

The DS-MWBFL can be transformed into a single spacing MWBFL (SS-MWBFL) by just a simple swapping of the common port and the 50% port of coupler 2 (C2). The residual first BS (thick solid arrow) that is exiting port 3 of circulator 2 will propagate from 50% into the common port of coupler 2. This first BS will circulate in the first loop of the cavity in a clockwise direction and re-enters the BGM to generate the second BS (thick dashed arrow).

The cascading process will continue to generate an SS-MWBFL where its output can be observed at OSA 1.

For pulsed laser generation, the home-fabricated multiwalled CNT (MWCNT)^[24] is placed into the ring cavity, in between the EDF and BGM. The fabricated SA is constructed by sandwiching an MWCNT polyethylene oxide (MWCNT-PEO) film of (2 mm × 2 mm) between two fiber connectors. The SA has an insertion loss of 3 dB and a transmission of 75% at 1563 nm. A noticeable band at 1530 nm⁻¹ can be seen from the Raman spectrum, and this confirms that the SA is multiwalled. The output spectrum of the pulsing is tapped out at the 10% port of the 10 dB coupler and monitored at OSA 2. The pulsing characteristics are further characterized by an oscilloscope (OSC, Tektronix TDS3052C) through a 1.2 GHz bandwidth photodetector (Thorlabs DET01CFC).

When no BP is injected into the cavity, unstable oscillation is observed in the range of 1570–1580 nm due to mode competition between different wavelengths. The free running cavity modes need to be suppressed in order to produce a stable MWBFL. Therefore, the BP is set at 1575 nm and amplified up to 13 dBm in this experiment. Figure 2 shows the output spectrum of the DS-MWBFL at three different 1480 nm pump powers, which are collected from OSA 1. A comb of lines is generated due to the cascading effect with the condition that the threshold condition is satisfied. A total of five lines are observed at the pump power of 165 mW. At the pump power of 70 mW, a stable first BS is observed at a peak power of -8 dBm at a wavelength 1575.08 nm, as depicted in Fig. 2. As the pump power is further increased to 120 mW, the third BS rises, and, as the pump power is further raised to 165 mW, the fifth and seventh BS can be seen at OSA 1. More BSs are produced at a higher pump power because of the higher gain provided by the erbium fiber, which assists the BS in reaching their SBS threshold. The anti-Stokes line is also observed at wavelengths shorter than BP, which occurs due to the FWM process. FWM is a nonlinear process where various Stokes waves interact with the pump wave to produce new wavelengths with lower power.

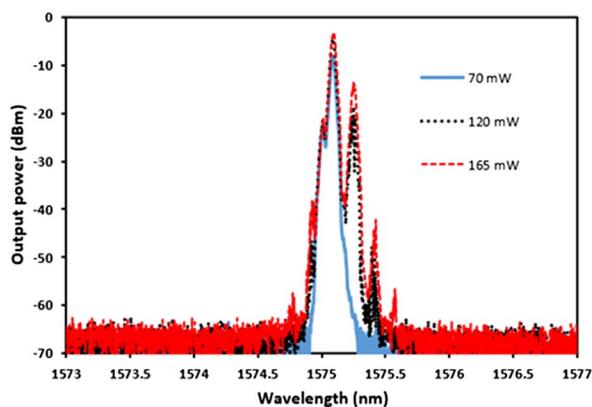


Fig. 2. (Color online) Output spectrum of DS-MWBFL (odd order) at OSA 1.

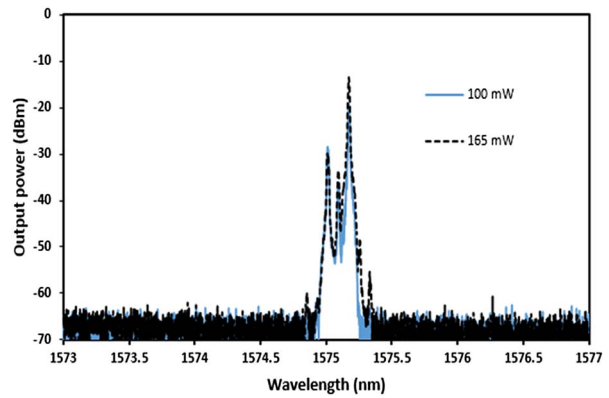


Fig. 3. (Color online) Output spectrum of DS-MWBFL (even order) at OSA 2.

The spacing between two consecutive Stokes and anti-Stokes is constantly measured at 0.016 nm. The even-order Stokes is tapped out at OSA 2 through the 10 dB coupler. Figure 3 shows the growth of the double spacing even-order Stokes at two different pump powers. The second BS of peak power -13.4 dBm is located at a wavelength of 1575.16 nm when the pump power is set to 100 mW. The fourth BS grows at the pump power of 165 mW. The spacing between the consecutive even-order BS is ascertained at 0.16 nm. A small portion of the first-order Stokes can be seen at a wavelength of 1575.08 nm with a peak power of -35 dBm. It is suspected that there is some leakage of signal at coupler 2, which results in the first BS traveling in both the counter clockwise and clockwise directions. As the first BS exits the port 3 circulator 2 and enters the 50% port of coupler 2, the first BS signal leaks into the other 50% port of coupler 2. The leaked first BS then travels into circulator 2, coupler 1, EDF, and BGM and, finally, is tapped out by the 10 dB coupler into OSA 2.

The DS-MWBFL can easily be converted to the SS-MWBFL by swapping the common and 50% port of coupler 2 (C2). Figure 4 shows the SS-MWBFL at three different pump powers, which is extracted at OSA 1. The first BS grows at the pump power of 85 mW, with a peak power of -2.3 dBm at 1575.08 nm. The second and third

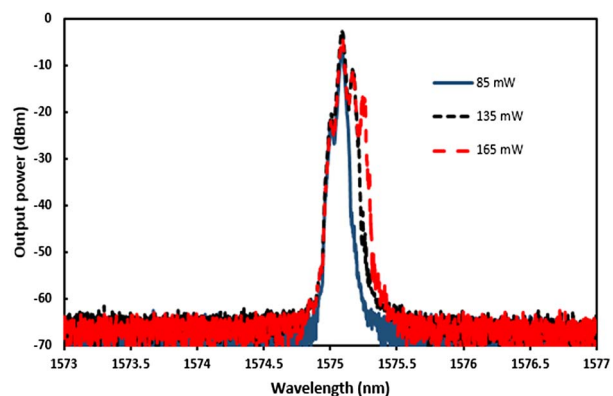


Fig. 4. (Color online) Output spectrum of SS-MWBFL at OSA 1.

BSs grow at the threshold pump powers of 135 and 165 mW, respectively. Fewer single spacing BSs are observed compared to the double spacing BS at OSA 1. This is attributed to spectral leakage, which happens at coupler 2. Ideally, 100% of the first BS should be coupled into the common port of coupler 2. However, a portion of the first BS is leaked into the other 50% port of coupler 2. As a result, the optical power of the first BS, which enters the common port and travels in the clockwise direction, drops. Hence, this first BS acquires higher threshold power to trigger the generation of the subsequent BS. This explains why fewer Stokes lines are observed here. Over the other end at OSA 2, only the BP signal at 1575 nm is detected. The leaked first BS, which propagates in the counter clockwise direction and goes into the BGM, does not have ample power to trigger subsequent Stokes. The method that is proposed here to perform switchable single and double BS is different compared to the work demonstrated by Zhou *et al.*^[14]. In this experiment, both single and double BS travel within the dual loop of the cavity, while in the experiment demonstrated by Zhou *et al.*, single and double BS travel in two and one loops of the cavity, respectively.

Pulsing behavior is observed for DS- and SS-MWBFL at OSA 2. A strong fluctuation is observed at the OSC. The pulsing is further investigated by inserting a homemade MWCNT SA between the EDF and BGM. Figure 5 shows the temporal characteristic of the pulsed Brillouin MWBFL with CNT SA. The oscillation trace at the OSC shows constant peak-to-peak spacing of 35.7 μs , which translates to a repetition rate of 28 kHz. The measured pulse width at the OSC is ascertained at 10.8 μs . The peak amplitude of the oscillation trace oscillates from 12 to 26 mV. With the insertion of the CNT SA, the fluctuation at the OSC is observed to be reduced.

The TLS is then turned off, and the position of SA in the cavity is maintained. Pulsing is initiated as the pump power is raised to 110 mW, and its output spectrum is as depicted in Fig. 6. The optical signal now travels only within the first loop of the cavity. This is achieved by exploiting the intensity dependent and nonlinear optical absorption characteristics of the fabricated SA. With the TLS turned off, the lasing wavelength broadens compared to without the insertion of SA and is shifted to the 1558 nm region. The spectrum broadens due to self-phase

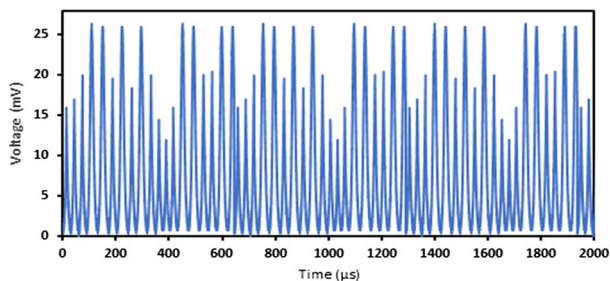


Fig. 5. Pulse train of Brillouin EDFL-based MWCNT SA.

modulation (SPM) and cross-phase modulation (XPM), and this will force the lasing wavelength to shift in order to support the broadening. The performance of this pulsed EDFL is further investigated with the OSC and radio frequency spectrum analyzer (RFSA). Figure 7 shows the temporal characteristic of the pulsed EDFL with constant peak-to-peak spacing of 40.5 μs , which translates to a repetition rate of 24.7 kHz. The measured pulse width at the OSC is ascertained at 9.6 μs . The inset of Fig. 7 reveals the RF spectrum of the pulsed EDFL, with the signal-to-noise ratio (SNR) observed to be more than 20 dB and the repetition rate at 24.7 kHz. As the pump power is further increased, the repetition rate of the laser is found to be

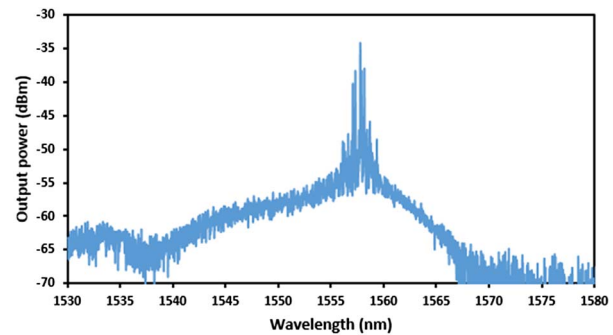


Fig. 6. Pulsed EDFL-based MWCNT SA.

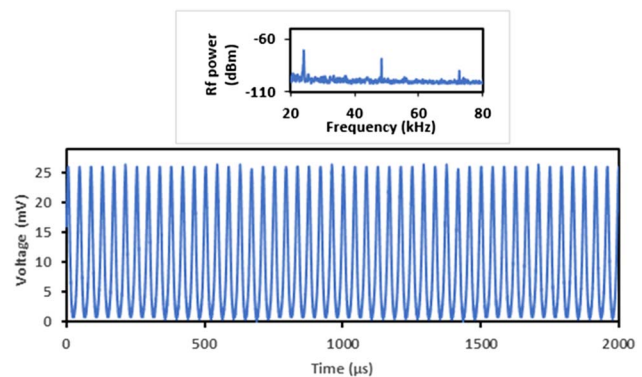


Fig. 7. Pulse train and RF spectrum of pulsed EDFL.

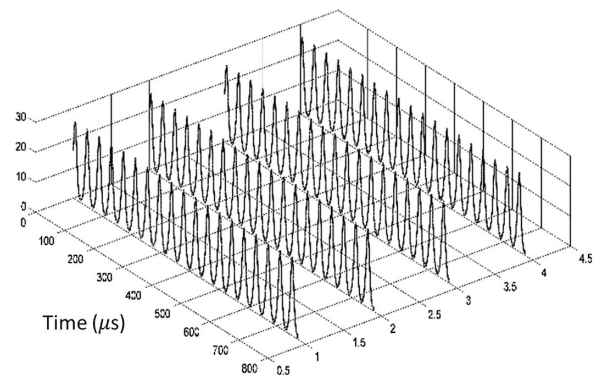


Fig. 8. Pulse train and RF spectrum of pulsed EDFL.

around 24.7 kHz, and this indicates that the laser is operating at its fundamental repetition rate. The pulse stability is also evaluated by scanning the oscillation trace for every one second. Referring to Fig. 8, it is found that the peak voltage of the pulse is stable at 26 mV.

In conclusion, switchable double and single MWBFL is successfully demonstrated. Brillouin switching is realized by swapping the 50% and common port of circulator 2. The number of multiwavelength lasings can be increased by using a higher power laser diode and by minimizing the optical component loss. The existing MWBFL cavity can be used for pulsed laser generation by inserting home-made CNT SA in between the EDF and BGM. The pulsed laser operates at a fundamental repetition rate of 24.7 kHz and a pulse width of 9.6 μ s. The proposed EDFL configuration is very flexible with multiple functions and can be used for various applications.

References

1. M. H. Al-Mansoori, M. K. Abd-Rahman, F. R. Mahamd Adikan, and M. A. Mahdi, *Opt. Express* **13**, 3471 (2005).
2. X. Bao, D. J. Webb, and D. A. Jackson, *Opt. Lett.* **18**, 552 (1993).
3. Y. Li, Y. G. Liu, J. B. Xu, B. Y. Tai, and Z. Wang, *Laser Phys.* **20**, 528 (2010).
4. X. S. Liu, L. Zhan, X. Hu, H. G. Li, Q. S. Shen, and Y. X. Xia, *Opt. Commun.* **282**, 2913 (2009).
5. N. A. Cholan, M. H. Al-Mansoori, A. S. M. Noor, A. Ismal, and M. A. Mahdi, *Opt. Express* **21**, 6131 (2013).
6. X. H. Feng, H. Y. Tam, H. L. Liu, and P. K. A. Wai, *Opt. Commun.* **268**, 278 (2006).
7. G. J. Cowle and D. Y. Stepanov, *Opt. Lett.* **21**, 1250 (1996).
8. M. N. M. Nasir, M. H. Al-Mansoori, H. A. A. Rashid, P. K. Choudhury, and Z. Yusoff, *Laser Phys.* **18**, 446 (2008).
9. A. W. Al-Alimi, N. A. Cholan, M. H. Yaacob, and M. A. Mahdi, *Laser Phys.* **26**, 065102 (2016).
10. B. A. Ahmad, A. W. Al-Alimi, A. F. Abas, S. W. Harun, and M. A. Mahdi, *Laser Phys.* **22**, 977 (2012).
11. X. Wang, Y. Yang, M. Liu, Y. Yuan, Y. Sun, Y. Gu, and Y. Yao, *Appl. Opt.* **55**, 6475 (2016).
12. L. Qian, D. Fen, H. Xie, and J. Sun, *Opt. Commun.* **340**, 74 (2015).
13. K. Hu, I. V. Kabakova, S. Lefrancois, D. D. Hudson, S. He, and B. J. Eggleton, *Opt. Express* **22**, 31884 (2014).
14. X. Zhou, K. Hu, Y. Wei, M. Bi, and G. Yang, *Laser Phys.* **27**, 015103 (2017).
15. V. L. Iezzi, T. F. S. Buttner, A. Tehranchi, S. Loranger, I. V. Kabakova, B. J. Eggleton, and R. Kashyap, *New J. Phys.* **18**, 055003 (2017).
16. A. Tehranchi, V. L. Iezzi, S. Loranger, and R. Kashyap, *IEEE J. Quantum Electron.* **52**, 9 (2016).
17. C. Montes, D. Bahloul, I. Bongrand, J. Botineau, G. Cheval, A. Mamhoud, E. Picholle, and A. Picozzi, *J. Opt. Soc. Am. B* **16**, 932 (1999).
18. K. Ogusu, *Opt. Rev.* **8**, 358 (2001).
19. Z. Sun, T. Hasan, F. Wang, A. G. Rozhin, I. H. White, and A. C. Ferarri, *Nano Res.* **3**, 404 (2010).
20. S. Y. Choi, H. Jeong, B. H. Hong, F. Rothermund, and D. I. Yeom, *Laser Phys. Lett.* **11**, 015101 (2014).
21. H. Liu, X.-W. Zheng, M. Liu, N. Zhao, A.-P. Luo, Z.-C. Luo, W.-C. Xu, H. Zhang, C.-J. Zhao, and S.-C. Wen, *Opt. Express* **22**, 6868 (2014).
22. J. Sotor, G. Sobon, M. Kowalczyk, W. Macherzynski, P. Paletko, and K. M. Abramski, *Opt. Lett.* **40**, 3885 (2015).
23. A. Zarei, Z. C. Tiu, F. Ahmad, H. Ahmad, and S. W. Harun, *IET Optoelectron.* **9**, 96 (2015).
24. F. Ahmad, H. Haris, R. M. Nor, N. R. Zulkepely, H. Ahmad, and S. W. Harun, *Chin. Phys. Lett.* **31**, 034204 (2014).